ACS APPLIED MATERIALS & INTERFACES

Letter

www.acsami.org

Piezoelectric Nanoparticle–Polymer Composite Foams

William R. McCall,[†] Kanguk Kim,[‡] Cory Heath,[†] Gina La Pierre,[†] and Donald J. Sirbuly*[,†,‡]

[†]Department of NanoEngineering and [‡]Materials Science and Engineering, University of California, San Diego, La Jolla, California 92093, United States

Supporting Information

ABSTRACT: Piezoelectric polymer composite foams are synthesized using different sugar-templating strategies. By incorporating sugar grains directly into polydimethylsiloxane mixtures containing barium titanate nanoparticles and carbon nanotubes, followed by removal of the sugar after polymer curing, highly compliant materials with excellent piezoelectric properties can be fabricated. Porosities and elasticity are tuned by simply adjusting the sugar/polymer mass ratio which gave an upper bound on the porosity of 73% and a lower bound on the elastic coefficient of 32 kPa. The electrical performance of the foams showed a direct relationship between porosity and the piezoelectric outputs, giving piezoelectric coefficient values of ~112 pC/N and a power output of ~18 mW/cm^3 under a load of 10 N for the highest porosity samples. These novel materials should find exciting use in a variety of applications including energy scavenging platforms, biosensors, and acoustic actuators.

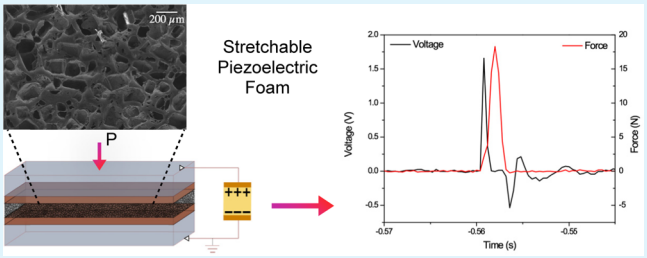

KEYWORDS: *piezoelectric, nanoparticle, foam, composite, $BaTiO_3$, polymer*

Mechanically flexible piezoelectric materials are highly sought after when building advanced sensors, actuators, and energy scavenger devices. The most common piezoelectric materials used in applications are focused on electroceramic thin films made from lead zirconate titanate ($Pb(Zr_xTi_{x-1})O_3$, also known as PZT) or barium titanate ($BaTiO_3$,BTO). Although these materials can have large piezoelectric moduli (d_{33}, which is the induced polarization along the poled axis over the applied stress along the same axis), with PZT reaching values >300 pC/N[1] and BTO exceeding 200 pC/N depending on ceramic type and processing conditions,[2,3] as thin films they are extremely brittle and difficult to shape into highly mechanically compliant structures. Improving mechanical flexibility of piezoelectrics, and creating higher order structures, is critical for driving new applications such as biological energy harvesting, compact acoustic transducers, and *in vivo* biodiagnostics. In recent years, there has been significant progress on making brittle electroceramics such as PZT more flexible by reducing the size of the piezoelectrics and fabricating high density arrays.[4,5] For example, McAlpine et al. demonstrated that PZT nanoribbons could be patterned on elastomers over large areas while maintaining effective piezoelectric coefficients of >100 pC/N for efficient energy scavenging devices.[4] Similar materials could also be suspended across trenches to probe cellular deformation with nanonewton force resolution.[6] Beyond perovskite-based ceramics, piezoelectric semiconductor oxides such as ZnO nanowire arrays have also been heavily researched for various applications including energy harvesting,[7,8] electronics,[9] and sensing.[10] However, systems that rely on one-dimensional nanostructures to enhance mechanical flexibility limit the number of stress directions which can produce piezoelectric fields. If structures can be fabricated with higher piezoelectric symmetry (i.e., macroscopic structure is similar in all direction), and more mechanically compliant materials, it is anticipated that the piezoelectric sensitivity will increase which will lead to a host of exciting applications.

Foams, which are basically intact materials with large void fractions (e.g., 50–80% air), offer a unique means of creating materials with similar structuring in all dimensions. Most foams can be considered a solid (or liquid) material with a random network of air channels. For piezoelectrics this typically involves generating ceramic materials through fused-deposition[11] or robocasting[12] techniques which can be refined to create well-controlled porous structures either by layer-by-layer or polymeric templating.[13] Interestingly, it was found that the PZT foams have higher piezo-sensitivity, lower acoustic impedance, and higher mechanical flexibility compared to their thin film counterparts, which have inspired a host of applications including wide-band hydrophones, actuators, and high-temperature filters.[14−16] Although porosity enhances many of the electrical and mechanical properties of electroceramics, they are still very brittle and cannot be strained beyond a few percent. Therefore, it is of interest to investigate alternative materials that can offer high piezoelectric coefficients while maintaining elasticity and isotropic mechanical integrity, as well as cost-effective synthetic strategies.

Of the many piezoelectric material types, polymers have not been as heavily researched compared to the electroceramics but can offer many advantages over ceramics including solution-based processability, biocompatibility, and high elasticity. The

Received: September 17, 2014
Accepted: October 29, 2014
Published: October 29, 2014

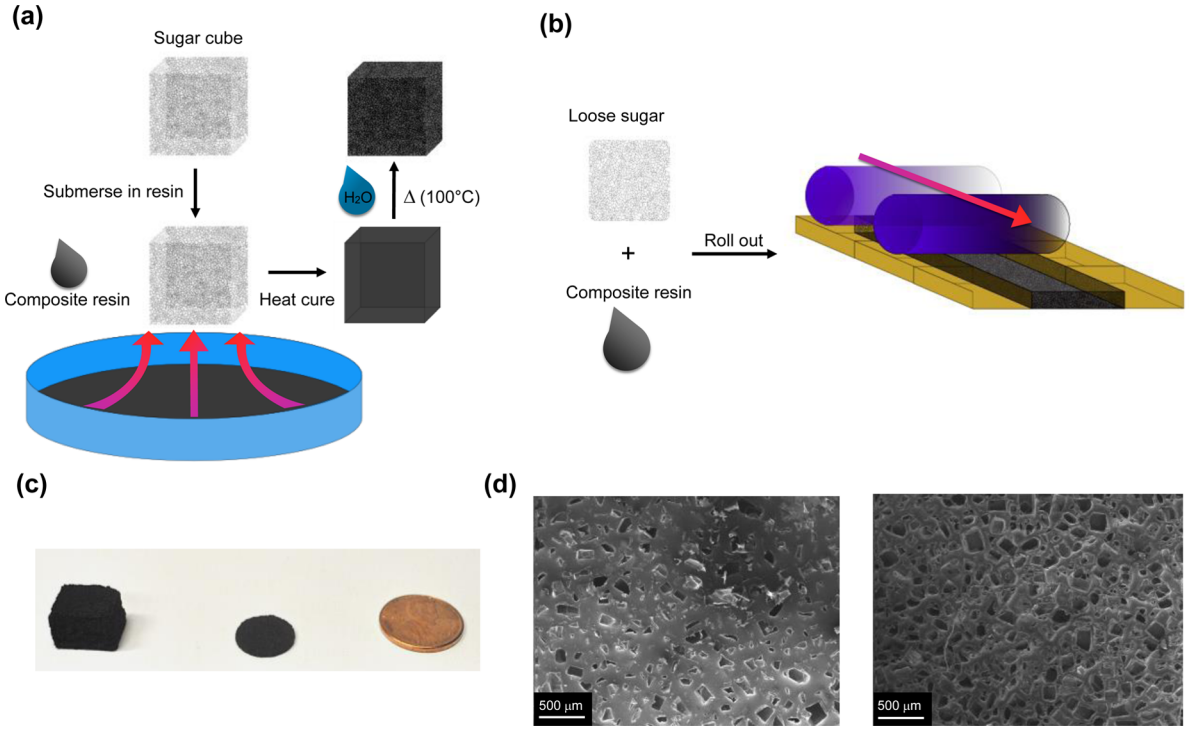

Figure 1. (a, b) Schematics of the (a) capillary-action and (b) roll-out methods of creating PNPFs. (c) Digital images of PNPFs created with the capillary-action method (left) and the roll-out method (middle). (d) Scanning electron micrographs of a 50% (left) and 73% (right) PNPF fabricated from the roll-out method using the same sugar grain size.

most well-known piezoelectric polymer is polyvinylidene fluoride (PVDF)[17] which has a piezoelectric coefficient (d_{33} ≈ −20 to −34 pC/N) that is about an order of magnitude smaller than PZT. Because of its electrical and mechanical properties, PVDF is being pursued for a wide range of applications including nonvolatile low voltage memory,[18] hydrophones and acoustic transmitters,[19,20] and implantable medical devices.[21] To improve flexibility and integration capability, PVDF can be electrospun into fibers, which has led to various energy harvesting devices.[22−24] PVDF foams with similar piezoelectric coefficients to the thin films and fibers have also been investigated; leading to efficient energy harvesters for sound.[25] Beyond the pure polymers such as PVDF, there have been advances with other polymer systems such as piezoelectric composites that combine electroceramic nanoparticles with a polymer matrix. For example, Lee et al. demonstrated that BTO nanoparticles could be mixed with an elastomer such as polydimethylsiloxane (PDMS) and carbon nanotubes (CNTs) to create highly flexible and efficient piezoelectric materials for energy harvesting.[26] The role of the CNTs in these composites was to enhance the stress transfer from the polymer to the BTO nanoparticles. Our group has further advanced these types of composite materials by demonstrating that they can be optically printed into user-defined 2D and 3D microstructures with strong piezoelectric properties.[27]

In this work, we investigate strategies to create highly elastic piezoelectric polymers that maintain 3D structural isotropy and strong piezoelectric behavior. Our approach combines simple foam processing with piezoelectric polymer composites so we can control the mechanical and electrical properties of the materials. Over the past few years researchers have been investigating porous elastomers such as PDMS for membrane separation and oil absorbent applications.[28−30] Of the various fabrication techniques for producing PDMS foams, the sugar-template method described by Choi et al. provides a simple and cost-effective procedure to make highly porous polymer materials.[29] A variant of ancient casting methods, here commercially available sugar is added to the PDMS mixture which can then be easily removed by soaking in water, leaving a 3D isotropic network of air channels in the polymer. The porous materials created with this method are extremely soft with an elastic modulus of ∼20 kPa which is well over an order of magnitude smaller than bulk PDMS (∼750 kPa). Here we leverage similar sugar-templating strategies to fabricate piezoelectric nanoparticle−polymer composite foams (PNPFs) and systematically study their porosity and mechanical properties and correlate these with the piezoelectric performance of the materials.

We investigated two variants of the foam process. In the first method cubed sugar is placed into a mixture of PDMS loaded with 10% BTO nanoparticles (diameter ∼80 nm) and 1% multiwalled CNTs (see the Supporting Information for experimental details) and the solution is allowed to infiltrate the void space of the sugar via capillary action (Figure 1a). Once the composite is cured, the sugar is removed by soaking the cube in boiling water. This method works well for creating large volume foam structures, but the limitations of the technique include not being able to fine-tune the porosity and it is challenging to generate high electric fields across the material to align the dipoles in the BTO nanoparticles without signficantly compressing the material or using extremely high voltatges (>10 kV). To better control the porosity and allow thinner films to be fabricated with higher throughput, free sugar can be added directly to the uncured polymer composite and rolled out once the proper viscosity is reached (Figure 1b). The porosity is tuned by simply adding different weight percents of the sugar. For example, sugar/polymer ratios ranging from 1.8 to 4.4 produced porous structures with an air fraction of 48.8%

to 73.7%, respectively (see the Supporting Information, Figure S1). Lower porosities were difficult to achieve since the materials would contain trapped pockets of sugar which could not be removed. The pore size is governed by the sugar grain size and can be kept constant by infusing the same sugar type regardless of the sugar/polymer ratio (Figure 1d). To limit pore size distribution we only used fine baker's sugar. Other sugar types (e.g., powdered, granulated) were experimented with, but ultimately led to inferior or unusable materials. As expected, the foam stiffness is directly related to porosity showing elastic moduli ranging from 248 kPa for the 50% porous composites to 32 kPa for the foams with 73% porosity (see the Supporting Information, Figure S2). The composite foams show slightly higher stiffness values compared to pure PDMS foams due to the addition of BTO nanoparticles and CNTs. The foams also show excellent cyclability (see the Supporting Information, Figure S3) without any signficant change in the elastic properties after repeated strain curves (1,200 cycles). This is important for piezoelectric applications that require repeated compression or tension to generate charge and power.

The as-made foams are only weakly piezoelectric, or show no piezoelectric properties, since the dipoles in the BTO nanoparticles are randomly oriented. To activate the material, the foams must be poled in an electric field larger than coercive field (~10 V/μm) of the BTO nanoparticles. This was achieved by depositing Au/Ti (10 nm Ti followed by 200 nm of Au) on a flexible Kapton substrate and interfacing the electrodes with the top and bottom surfaces of the foam and poling on a 150 °C hot plate for up to 15 h to ensure a fully polarized foam (Figure 2a). A thin (~5 μm) layer of cured PDMS was placed on the metal electrode prior to contacting with the foam to help eliminate shorting during poling. The piezoelectric charge coefficient (d_{33}) of the individual foams was quantified using a homemade piezoelectric test apparatus that reads out the voltage output of the material simultaneously with the applied load (see the Supporting Information, Figure S4). The instrument was fully calibrated using a commercial PZT film with a piezoelectric coefficient of 300 pC/N prior to testing the foams. Figure 2b,c shows some cycling data of a 73% foam and the measured effective d_{33} values as a function of porosity. At 0% porosity (i.e., neat film) the composites show only a weak piezoelectric coefficient of 6 pC/N but by 50% porosity the value has more than doubled, eventually reaching ~112 pC/N at a porosity of 73%. The larger error in the piezoelectric coefficient (and strain rate in Figure 3b) at higher porosities is likely due to an increased contribution to the electrical output from shear and/or bending modes that can slightly vary between runs when measuring a more compliant material. With only 10% loading of the BTO nanoparticles, and CNTs added to enhance the mechanical-to-electrical conversion process, these values at high porosity are significantly larger than pure polymers such as PVDF. We believe the enhanced piezoelectric properties of the foam structure are due to a combination of effects that include being a softer material (i.e., smaller loads required to strain the material) compared to the 0% films and

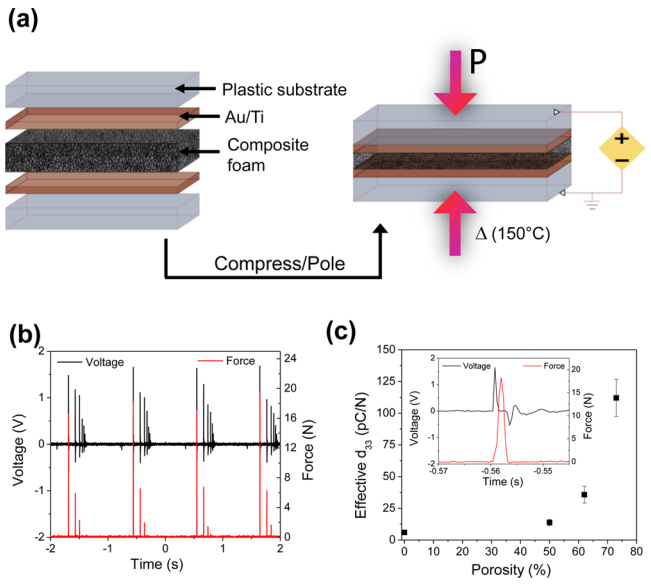

Figure 2. (a) Schematic of the poling process. Not shown are the thin (~5 μm) PDMS layers on the Au/Ti electrode to eliminate shorting during the poling process. To increase the poling field using a static voltage the foams can be compressed. (b) Cycling data for a 73% foam showing the piezoelectric output and applied force vs time as a rod is dropped (and allowed to bounce) on the foam 4 times. (c) Effective piezoelectric coefficient (d_{33}) of the PNPFs as a function of porosity. The neat film (0% porosity) is also shown for comparison. Data points are the average of 5 measurements and the error bars are the spread in the data. (Inset) Zoom in on one of the output cycles in (b) showing the piezoelectric response of the foam as a function of time and applied force.

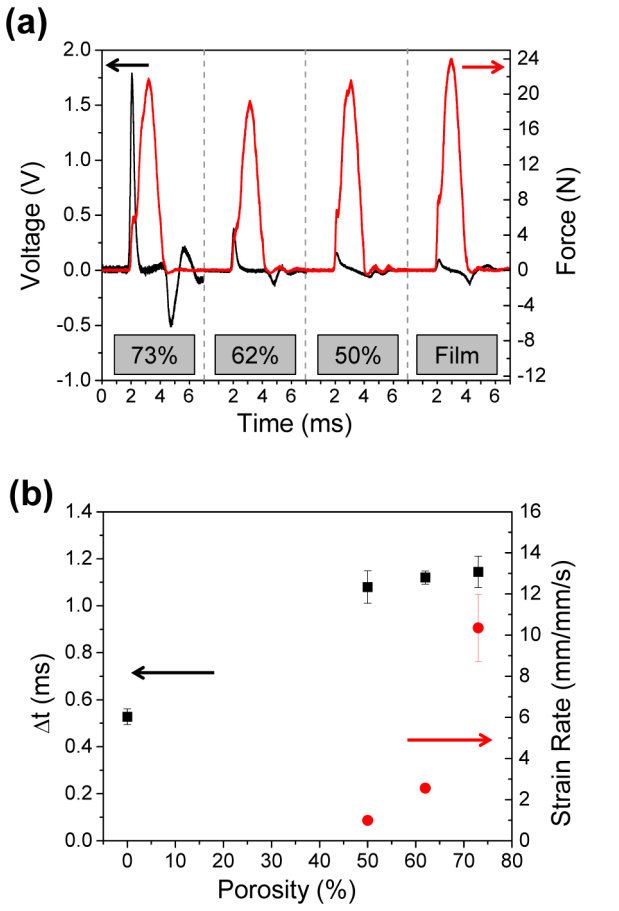

Figure 3. (a) Single charge/discharge traces (7 ms each) for a 0% (neat film), 50%, 62%, and 73% porous film. The applied force is also plotted in real−time. (b) Time difference between peak voltage and force as a function of porosity. Also plotted is the compressive strain rate of the foam as a function of porosity under an ~10 N load.

dx.doi.org/10.1021/am506415y | ACS Appl. Mater. Interfaces 2014, 6, 19504−19509

that the interconnected polymer matrix is helping to localize stresses on the piezoelectric nanoparticles. To boost the piezoelectric output further, various strategies can be employed such as direct grafting of the BTO nanoparticles to the polymer chains,[27] using piezoelectric nanoparticles with higher intrinsic d_{33} values (e.g., PZT), or increasing the nanoparticle loading percent.

It is important when dealing with high surface area materials to properly decouple the piezoelectric effects from other charge forming processes such as the triboelectric effect. It has been shown that when materials (e.g., polymers) with different contact charging properties are interfaced, they can produce large static-charge driven signals while in physical contact.[31] This triboelectric effect is even further enhanced when two materials at different regions of the tribo-series are roughened and then brought together.[32] Similar to a reduction−oxidation potential, the further the materials are away from each other on a triboelectric scale, the larger the electrostatic potentials will be when the two materials come in contact. It is expected that there will be strong triboelectric effects for devices that contain a high surface area PDMS foam in contact with an electrode. We investigated this and found that the pure PDMS foams produced recordable triboelectric responses when a load is applied to the foam (see the Supporting Information, Figure S5). When the unpoled piezoelectric composite foams were tested with pure PDMS coatings on the electrodes there were still measurable static potentials. However, the triboelectric effect could be suppressed by first poling with the pure PDMS coatings and then switching to unpoled composite layers (~5 μm thick) on the electrodes. This minimizes the difference on the tribo-scale and allowed the piezoelectric properties to be probed independently from contact charging effects.

With such large surface-to-volume ratios, it is likely that the charging dynamics of the foams will be different depending on the porosity. To investigate this we tracked both the applied force and voltage output of the foam in real-time. Figure 3a captures single charging and discharging cycles for a neat film and samples with different porosity. As force is applied to the foam, the material is compressed which strains the BTO nanoparticles, causing a recordable piezoelectric potential across the foam. For an ideal piezoelectric material (i.e., one that can efficiently hold charge over time) the voltage should peak at max force, but if charge is lost too quickly there will be an offset between the max voltage and max force. This can be clearly seen with the foams when plotting the time difference (Δt), defined as the time delay between when the max voltage and force are recorded, as a function of porosity (Figure 3b). Before the maximum force is attained, the porous materials have already lost most of their charge. This suggests that the PNPFs are poor capacitors and that we could be underestimating the piezoelectric coefficients for our materials. To get smaller Δt values, higher strain rates need to be used but under the current loading experiments, we are only able to attain strain rates of up to ~10 s^{-1} (see the Supporting Information for details on calculating strain rate). Future work will investigate how strain rate and frequency can be used to tune the piezoelectric response of the PNPFs and we will explore ways of impoving electrical capacitance of the porous materials (e.g., different electrodes, foam passivation layers, etc.). A closer look at the foam cycling curves also supports the claim of a charging/discharging process that is strongly dependent on the strain rate. For the neat film, their exists a predominant charge and discharge trace that has much better symmetry compared to the porous films. This is due to the similar strain rates during compression and recovery. However, for the foams, the charge cycle peaks at a much larger value compared to the discharge. This can be explained by the slow elastic recovery of the foam materials after compression, which results in a much smaller strain rate and weaker discharge signal.

To understand the power generating capabilities of these PNPFs subject to mechanical stimulation we created a simple circuit where the devices were connected to a potentiometer in series and the resulting power output was measured across the external component. The foams were cycled with ~10 N loads and the resulting power densities are plotted in Figure 4a.

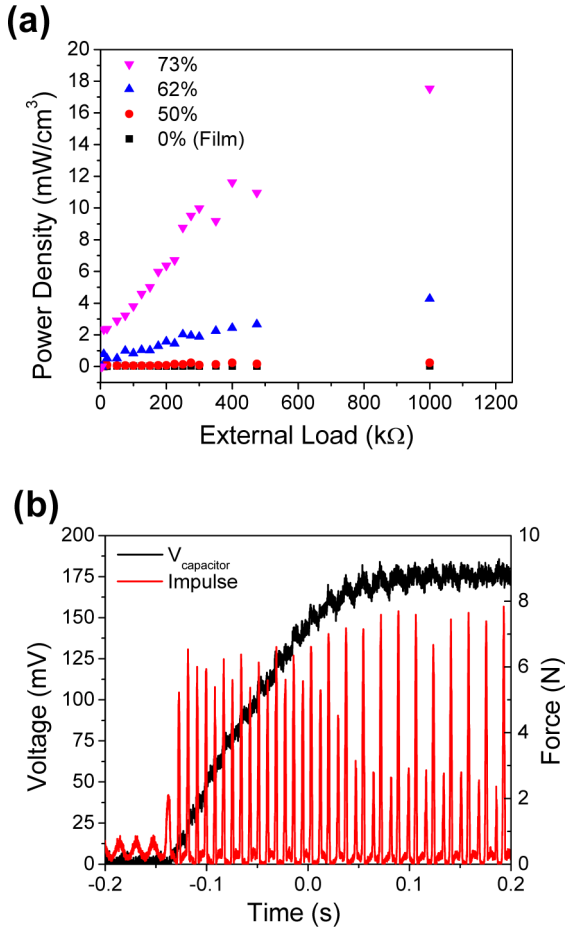

Figure 4. (a) Power output as a function of external load for different porosity films and a neat film. A ~ 10 N load is being applied to the samples. (b) Plot showing the charging up of a 100 nF capacitor. The voltage and 118 Hz impulse force are plotted as a function of time.

Under small external loads we see the lowest power output, but once the load is increased to values above ~10 kΩ the power density steadily climbs to ~18 mW/cm^3 for the highest porosity samples and then plateaus. This trend fits the electronic model of an ideal capacitor which has infinite impedance. In order to maximize power transfer from the piezoelectric device to a load resistor the impedances of both must be matched. Since the foams are essentially high impedance, parallel plate capactitors with air as the dielectric, it is expected that the foams will produce the highest power densities under higher electrical loads. In addition to measuring the power output under varying external loads, the ability of the

PNPFs in charging up a capacitor was investigated. The device was connected to a simple rectifying circuit, which included a 100 nF charging capacitor, and subjected to a cycling load of ~8 N at 118 Hz. The voltage across the capacitor, and the impulse train, were recorded with time (Figure 4b) and showed a maximum voltage of ~175 mV after ~200 ms. Because of the quick charging and discharging capability of the device it is expected that higher frequency stimuli under smaller loads will produce faster capacitor charging times and larger voltages.

In summary, we have utilized simple sugar-templating methods to fabricate piezoelectric polymer composite foams. Two strategies were laid out for creating porous piezoelectric polymers including a capillary-action and roll-out method. The roll-out process allowed much finer control over the porosity, enabled much thinner films, and has the potential to be scaled up to fabricate material over large areas. The mechanical studies showed the anticipated trend of lower elastic coefficients at higher porosity, whereas the piezoelectric properties were signicantly boosted when the air fraction was increased. Because of the large surface area of the foams, it was observed that charge across the foam could not be held as efficiently as the thin films, but created a much more sensitive material. Improvements on the capacitance and discharging dynamics of the foams should be attainable by leveraging different electrode interfaces, passivating layers, and/or composite materials that eliminate the CNTs. Power studies indicated that these materials can operate under mechanical loads and have enough power to drive low power devices. Given the tunable porosity, mechanical flexibility of the foams, high surface area, high piezoelectric sensitivity, isotropic microscture, and more biocompatible chemical makeup compared to the bulk electroceramics, these foams should find immediate applications in energy scavenging platforms, biosensors, and acoustic transducers.

■ ASSOCIATED CONTENT

Supporting Information

Experimental details, porosity data, stress/strain curves, schematics of piezo-testing apparatus, and triboelectric testing with different polymer coatings on the electrodes. This material is available free of charge via the Internet at http://pubs.acs.org.

■ AUTHOR INFORMATION

Corresponding Author

*E-mail: dsirbuly@ucsd.edu.

Notes

The authors declare no competing financial interest.

■ REFERENCES

(1) Jaffe, B.; Cook, W. R.; Jaffe, H. *Piezoelectric Ceramics*; Academic Press: London, 1971.

(2) Takahashi, H.; Numamoto, Y.; Tani, J.; Matsuta, K.; Qiu, J. H.; Tsurekawa, S. Lead-Free Barium Titanate Ceramics with Large Piezoelectric Constant Fabricated by Microwave Sintering. *Jpn. J. Appl. Phys., Part 2* **2006**, *45*, L30−L32.

(3) Wada, S.; Yako, K.; Kakemoto, H.; Tsurumi, T.; Kiguchi, T. Enhanced Piezoelectric Properties of Barium Titanate Single Crystals with Different Engineered-Domain Sizes. *J. Appl. Phys.* **2005**, *98*, 014109.

(4) Qi, Y.; Jafferis, N. T.; Lyons, K., Jr.; Lee, C. M.; Ahmad, H.; McAlpine, M. C. Piezoelectric Ribbons Printed onto Rubber for Flexible Energy Conversion. *Nano Lett.* **2010**, *10*, 524−528.

(5) Xu, S.; Hansen, B. J.; Wang, Z. L. Piezoelectric-Nanowire-Enabled Power Source for Driving Wireless Microelectronics. *Nat. Commun.* **2010**, *1*, 1−5.

(6) Nguyen, T. D.; Deshmukh, N.; Nagarah, J. M.; Kramer, T.; Purohit, P. K.; Berry, M. J.; McAlpine, M. C. Piezoelectric Nanoribbons for Monitoring Cellular Deformations. *Nat. Nanotechnol.* **2012**, *7*, 587−593.

(7) Xu, S.; Qin, Y.; Xu, C.; Wei, Y. G.; Yang, R. S.; Wang, Z. L. Self-Powered Nanowire Devices. *Nat. Nanotechnol.* **2010**, *5*, 366−373.

(8) Wang, X. Y.; Kim, K.; Wang, Y. M.; Stadermann, M.; Noy, A.; Hamza, A. V.; Yang, J. H.; Sirbuly, D. J. Matrix-Assisted Energy Conversion in Nanostructured Piezoelectric Arrays. *Nano Lett.* **2010**, *10*, 4901−4907.

(9) Wang, Z. L. Progress in Piezotronics and Piezo-Phototronics. *Adv. Mater.* **2012**, *24*, 4632−4646.

(10) Wang, Z. L. Self-Powered Nanosensors and Nanosystems. *Adv. Mater.* **2012**, *24*, 280−285.

(11) Allahverdi, M.; Danforth, S. C.; Jafari, M.; Safari, A. Processing of Advanced Electroceramic Components by Fused Deposition Technique. *J. Eur. Ceram. Soc.* **2001**, *21*, 1485−1490.

(12) Tuttle, B. A.; Smay, J. E.; Cesarano, J.; Voigt, J. A.; Scofield, T. W.; Olson, W. R.; Lewis, J. A. Robocast $Pb(Zr_{0.95}Ti_{0.05})O_3$ Ceramic Monoliths and Composites. *J. Am. Ceram. Soc.* **2001**, *84*, 872−874.

(13) Rittenmyer, K.; Shrout, T.; Schulze, W. A.; Newnham, R. E. Piezoelectric 3−3 Composites. *Ferroelectrics* **1982**, *41*, 189−95.

(14) Kara, H.; Ramesh, R.; Stevens, R.; Bowen, C. R. Porous PZT Ceramics for Receiving Transducers. *IEEE Trans. Ultrason. Eng.* **2003**, *50*, 289−296.

(15) Bast, U.; Wersing, W. The Influence of Internal Voids with 3−1 Connectivity on the Properties of Piezoelectric Ceramics Prepared by a New Planar Process. *Ferroelectrics* **1989**, *94*, 229−242.

(16) Boumchedda, K.; Hamadi, M.; Fantozzi, G. Properties of a Hydrophone Produced with Porous PZT Ceramic. *J. Eur. Ceram. Soc.* **2007**, *27*, 4169−4171.

(17) Kawai, H. Piezoelectricity of Poly (Vinylidene Fluoride). *Jpn. J. Appl. Phys.* **1969**, *8*, 975−976.

(18) Hu, Z.; Tian, M.; Nysten, B.; Jonas, A. M. Regular Arrays of Highly Ordered Ferroelectric Polymer Nanostructures for Non-Volatile Low-Voltage Memories. *Nat. Mater.* **2009**, *8*, 62−67.

(19) Foster, F. S.; Harasiewicz, E. A.; Sherar, M. D. A History of Medical and Biological Imaging with Polyvinylidene Fluoride (PVDF) Transducers. *IEEE Trans. Ultrason. Eng.* **2000**, *47*, 1363−1371.

(20) Harris, G. R.; Preston, R. C.; DeReggi, A. S. The Impact of Piezoelectric PVDF on Medical Ultrasound Exposure Measurements, Standards, and Regulations. *IEEE Trans. Ultrason. Eng.* **2000**, *47*, 1321−1335.

(21) Wang, F.; Tanaka, M.; Chonan, S. Development of a PVDF Piezopolymer Sensor for Unconstrained in-Sleep Cardiorespiratory Monitoring. *J. Intell. Mater. Syst. Struct.* **2003**, *14*, 185−190.

(22) Chang, C. E.; Tran, V. H.; Wang, J. B.; Fuh, Y. K.; Lin, L. W. Direct-Write Piezoelectric Polymeric Nanogenerator with High Energy Conversion Efficiency. *Nano Lett.* **2010**, *10*, 726−731.

(23) Hansen, B. J.; Liu, Y.; Yang, R. S.; Wang, Z. L. Hybrid Nanogenerator for Concurrently Harvesting Biomechanical and Biochemical Energy. *ACS Nano* **2010**, *4*, 3647−3652.

(24) Persano, L.; Dagdeviren, C.; Su, Y.; Zhang, Y.; Girardo, S.; Pisignano, D.; Huang, Y.; Rogers, J. A. High Performance Piezoelectric Devices Based on Aligned Arrays of Nanofibers of Poly-(Vinylidenefluoride-Co-Trifluoroethylene). *Nat. Commun.* **2013**, *4*, 1−10.

(25) Cha, S.; Kim, S. M.; Kim, H.; Ku, J.; Sohn, J. I.; Park, Y. J.; Song, B. G.; Jung, M. H.; Lee, E. K.; Choi, B. L.; Park, J. J.; Wang, Z. L.; Kim, J. M.; Kim, K. Porous PVDF as Effective Sonic Wave Driven Nanogenerators. *Nano Lett.* **2011**, *11*, 5142−5147.

(26) Park, K.-I.; Lee, M.; Liu, Y.; Moon, S.; Hwang, G.-T.; Zhu, G.; Kim, J. E.; Kim, S. O.; Kim, D. K.; Wang, Z. L.; Lee, K. J. Flexible Nanocomposite Generator Made of $BaTiO_3$ Nanoparticles and Graphitic Carbons. *Adv. Mater.* **2012**, *24*, 2999−3004.

(27) Kim, K.; Zhu, W.; Qu, X.; Aaronson, C.; McCall, W. R.; Chen, S. C.; Sirbuly, D. J. 3D Optical Printing of Piezoelectric Nanoparticle-Polymer Composite Materials. *ACS Nano* **2014**, DOI: 10.1021/nn503268f.
(28) Park, I.; Efimenko, K.; Sjoblom, J.; Genzer, J. Rapid Removal of Organics and Oil Spills from Waters Using Silicone Rubber "Sponges". *J. Dispersion Sci. Technol.* **2009**, *30*, 318−327.
(29) Choi, S. J.; Kwon, T. H.; Im, H.; Moon, D. I.; Baek, D. J.; Seol, M. L.; Duarte, J. P.; Choi, Y. K. A Polydimethylsiloxane (Pdms) Sponge for the Selective Absorption of Oil from Water. *ACS Appl. Mater. Interfaces* **2011**, *3*, 4552−4556.
(30) Zhang, A. J.; Chen, M. J.; Du, C.; Guo, H. Z.; Bai, H.; Li, L. Poly(Dimethylsiloxane) Oil Absorbent with a Three-Dimensionally Interconnected Porous Structure and Swellable Skeleton. *ACS Appl. Mater. Interfaces* **2013**, *5*, 10201−10206.
(31) Diaz, A. F.; Felix-Navarro, R. M. A Semi-Quantitative Tribo-Electric Series for Polymeric Materials: The Influence of Chemical Structure and Properties. *J. Electrostatics* **2004**, *62*, 277−290.
(32) Fan, F.-R.; Lin, L.; Zhu, G.; Wu, W.; Zhang, R.; Wang, Z. L. Transparent Triboelectric Nanogenerators and Self-Powered Pressure Sensors Based on Micropatterned Plastic Films. *Nano Lett.* **2012**, *12*, 3109−3114.